J. Fluid Mech. (1977), *vol.* 81, *part* 4, *pp.* 625–640
Printed in Great Britain

Effect of tube elasticity on the stability of Poiseuille flow

By VIJAY K. GARG

Department of Mechanical Engineering, Indian Institute of Technology, Kanpur

(Received 6 August 1976)

The effect of tube elasticity on the stability of Poiseuille flow to infinitesimal axisymmetric disturbances is investigated. The disturbance equations for the fluid are solved numerically while those for the arbitrarily thick tube are solved analytically in terms of Bessel functions of complex argument. It is shown that an elastic tube can cause instability of Poiseuille flow, unlike a rigid tube, in which the flow is always stable. Neutral curves are presented for various values of the tube parameters. It is found that the critical Reynolds number varies almost as the square root of the Young's modulus of the tube material while the critical dimensionless frequency is almost invariant, being about 1·1 for the cases studied.

1. Introduction

Fluid flow over flexible boundaries has been a subject of study for the last two decades, starting with the work of Miles (1957) on the theory of water-wave generation by wind. Benjamin (1960) was perhaps the first to consider the effects of a flexible boundary on hydrodynamic stability. Since then, several studies have been made to determine the effects of wall flexibility on the stability of laminar boundary-layer flow (Landahl 1962; Benjamin 1963) and on the stability of plane Poiseuille flow (Hains & Price 1962*a*, *b*). These are summarized in a review article by Benjamin (1964).

Studies have also been carried out to find the modes of wave propagation in stationary fluids contained in a flexible tube. To that end Lin & Morgan (1956) and Rubinow & Keller (1971) present extensive mode analyses for inviscid fluids, while Cox (1969) summarizes the many analyses for plane-wave or lowest-mode propagation in viscous incompressible fluids. DeArmond & Rouleau (1972) found the lower modes for wave propagation in compressible viscous fluids and showed that tube elasticity was the primary factor in causing pressure–pulse dispersion.

While it has been confirmed that Poiseuille flow in a rigid circular tube is stable to all infinitesimal disturbances (Salwen & Grosch 1972; Garg & Rouleau 1972; Gill 1973), it has been found recently (Garg & Rouleau 1974) that flow in an elastic tube is unstable to infinitesimal axisymmetric disturbances. However, in that analysis the tube was modelled as a thin elastic membrane with mass, and so could not support shear or bending stresses.

In the present paper the tube is described by the differential equations of linear elasticity, so that it may be arbitrarily (though uniformly) thick and there is no limitation as to the stresses or the modes of propagation that may be present. The fluid is described by the usual linearized disturbance equations which follow from the Navier–Stokes and continuity equations. The analysis is developed for both

spatial and temporal stability of flow in a thick, arbitrarily constrained, linear, viscoelastic tube for which the Young's modulus is complex. In this paper, however, results are presented only for the linear spatial stability of flow in a purely elastic, unconstrained tube.

2. Analysis

2.1. *Fluid equations*

For an infinitesimal axisymmetric disturbance superimposed on Poiseuille flow in a circular tube, the linearized Navier–Stokes and continuity equations are made non-dimensional with respect to the mean inner radius a of the tube, the maximum velocity $\mathscr{V}$ of the Poiseuille flow and the density ρ of the fluid. Then each component, say $\phi(r,z,t)$, of the Fourier series forming the axisymmetric disturbance is assumed to be of the form

$$\phi(r,z,t) = \mathrm{Re}\,[\bar{\phi}(r)\exp(kz - i\omega t)], \tag{1}$$

where Re denotes the real part of a complex function, r, z and t are the dimensionless radial, axial and time co-ordinates, ω is the complex frequency and k is the complex wavenumber. For the analysis of spatial stability, ω is taken as purely real, and for temporal stability, k is taken as purely imaginary. Substitution of disturbance velocity components and pressure in the form (1) into the linearized continuity and Navier–Stokes equations leads to the following set of equations (Garg & Rouleau 1972):

$$\left(D + \frac{1}{r}\right)\bar{v}_r + k\bar{v}_z = 0, \tag{2a}$$

$$\left[D^2 + \frac{1}{r}D + \left\{k^2 - \frac{1}{r^2} - R(kV_z - i\omega)\right\}\right]\bar{v}_r - RD\bar{p} = 0, \tag{2b}$$

$$\left[D^2 + \frac{1}{r}D + \{k^2 - R(kV_z - i\omega)\}\right]\bar{v}_z - R\bar{v}_r DV_z - Rk\bar{p} = 0, \tag{2c}$$

where D is the operator d/dr, $\bar{v}_r$, $\bar{v}_z$ and $\bar{p}$ are the dimensionless complex eigenfunctions for the disturbance velocity components and pressure, $V_z = (1-r^2)$ is the dimensionless velocity of the Poiseuille flow and $R = a\mathscr{V}/\nu$ is the Reynolds number, where ν is the kinematic viscosity of the fluid and the maximum velocity $\mathscr{V}$ is twice the average velocity.

2.2. *Tube equations*

The tube is assumed to be an infinitely long circular cylinder made of a linear, isotropic, homogeneous, viscoelastic solid of arbitrary but uniform thickness. The perturbations from the state of rest of the tube are assumed to be infinitesimal and axially symmetric. The radial and axial displacements η_r and η_z, non-dimensionalized with respect to the inner radius a of the tube at rest, describe the motion of a particle in the tube from its rest position. For a tube with a Poisson ratio $\sigma \neq \frac{1}{2}$, these displacements satisfy the following non-dimensional equations of linear viscoelasticity (Love 1944):

$$\frac{\zeta(1-2\sigma)}{\xi(1-\sigma)^2}\frac{\partial^2\eta_r}{\partial t^2} = \left(\frac{\partial^2\eta_r}{\partial r^2} + \frac{1}{r}\frac{\partial\eta_r}{\partial r} - \frac{\eta_r}{r^2}\right) + \frac{(1-2\sigma)}{2(1-\sigma)}\frac{\partial^2\eta_r}{\partial z^2} + \frac{1}{2(1-\sigma)}\frac{\partial^2\eta_z}{\partial z\,\partial r}, \tag{3a}$$

$$\frac{2\zeta}{\xi(1-\sigma)}\frac{\partial^2\eta_z}{\partial t^2} = \left(\frac{\partial^2\eta_z}{\partial r^2} + \frac{1}{r}\frac{\partial\eta_z}{\partial r}\right) + \frac{2(1-\sigma)}{(1-2\sigma)}\frac{\partial^2\eta_z}{\partial z^2} + \frac{1}{(1-2\sigma)}\left[\frac{\partial^2\eta_r}{\partial z\,\partial r} + \frac{1}{r}\frac{\partial\eta_r}{\partial z}\right], \tag{3b}$$

where ζ is the ratio of the tube density ρ_w to the fluid density ρ, and ξ is given by

$$\xi = \frac{E}{\rho \mathscr{V}^2(1-\sigma^2)} = \frac{\zeta C_t^2}{1-\sigma^2}, \tag{4}$$

where E is Young's modulus and C_t is the dimensionless speed of sound ($= (E/\rho_w)^{\frac{1}{2}}/\mathscr{V}$) in the tube material. E is complex for a viscoelastic material but pure real for an elastic material. If η_r and η_z are expressed in the form (1), the equations of motion (3) reduce to

$$\left.\begin{aligned} \left[D^2+\frac{1}{r}D+\left(m^2-\frac{1}{r^2}\right)\right]\bar{\eta}_r+\frac{k}{2(1-\sigma)}[D\bar{\eta}_z-k\bar{\eta}_r] &= 0, \\ \left[D^2+\frac{1}{r}D+q^2\right]\bar{\eta}_z+\frac{k}{(1-2\sigma)}\left[k\bar{\eta}_z+\left(D+\frac{1}{r}\right)\bar{\eta}_r\right] &= 0, \end{aligned}\right\} \tag{5}$$

where

$$m^2 = k^2+\frac{\zeta\omega^2(1-2\sigma)}{\xi(1-\sigma)^2}, \quad q^2 = k^2+\frac{2\zeta\omega^2}{\xi(1-\sigma)}, \tag{6}$$

m and q showing the coupling between the disturbance and tube parameters.

For an incompressible material ($\sigma = \frac{1}{2}$), (3) and (5) are not valid owing to the factor $1-2\sigma$ in the denominator of certain terms. For this case, the tube equations corresponding to (3) are (Love 1944)

$$\frac{4\zeta}{\xi}\frac{\partial^2\eta_r}{\partial t^2} = \frac{\partial^2\eta_r}{\partial r^2}+\frac{1}{r}\frac{\partial\eta_r}{\partial r}-\frac{\eta_r}{r^2}+\frac{\partial^2\eta_r}{\partial z^2}-\frac{4}{\xi}\frac{\partial\beta}{\partial r}, \tag{7a}$$

$$\frac{4\zeta}{\xi}\frac{\partial^2\eta_z}{\partial t^2} = \frac{\partial^2\eta_z}{\partial r^2}+\frac{1}{r}\frac{\partial\eta_z}{\partial r}+\frac{\partial^2\eta_z}{\partial z^2}-\frac{4}{\xi}\frac{\partial\beta}{\partial z}, \tag{7b}$$

$$\frac{\partial\eta_z}{\partial z}+\frac{\partial\eta_r}{\partial r}+\frac{\eta_r}{r} = 0, \tag{7c}$$

where $\beta = \beta^*/(\rho\mathscr{V}^2)$, with β^* representing the difference between the mean pressure at any point of the tube in the strained state and the pressure at the same point in the unstrained state. Equation (7c) represents the condition of incompressibility, and ξ is still given by (4). If η_r, η_z and β are expressed in the form (1), equations (7) reduce to

$$\left[D^2+\frac{1}{r}D+\left(q^2-\frac{1}{r^2}\right)\right]\bar{\eta}_r-\frac{4}{\xi}D\bar{\beta} = 0, \tag{8a}$$

$$\left[D^2+\frac{1}{r}D+q^2\right]\bar{\eta}_z-\frac{4k}{\xi}\bar{\beta} = 0, \tag{8b}$$

$$\left(D+\frac{1}{r}\right)\bar{\eta}_r+k\bar{\eta}_z = 0, \tag{8c}$$

where

$$q^2 = k^2+4\zeta\omega^2/\xi. \tag{9}$$

It may be pointed out that the definition of q given by (9) is the same as that given by (6) for $\sigma = \frac{1}{2}$.

2.3. *Boundary conditions*

The physical restrictions at the centre of the tube require that the fluid velocity and pressure be bounded and continuous at $r = 0$. Therefore the boundary conditions at $r = 0$ are (Garg & Rouleau 1972)

$$\bar{v}_r(0) = 0, \quad \bar{v}_z(0) \text{ finite}, \quad \bar{p}(0) \text{ finite}. \tag{10}$$

The velocity of the fluid and of the wall must be continuous at the interface, i.e. at

$$r = 1 + \mathrm{Re}\,[\bar{\eta}_r \exp(kz - i\omega t)].$$

However, it is convenient to express this boundary condition at the location $r = 1$. Following Benjamin (1960), therefore, the fluid velocities are expanded in a Taylor series about $r = 1$. Retaining only the dominant terms of the series gives

$$\left.\begin{aligned} v_r &= \partial\eta_r/\partial t \\ \eta_r\, dV_z/dr + v_z &= \partial\eta_z/\partial t \end{aligned}\right\} \quad \text{at} \quad r = 1. \tag{11}$$

In view of (1), this reduces to

$$\left.\begin{aligned} \bar{v}_r + i\omega\bar{\eta}_r &= 0 \\ \bar{\eta}_r\, dV_z/dr + \bar{v}_z + i\omega\bar{\eta}_z &= 0 \end{aligned}\right\} \quad \text{at} \quad r = 1. \tag{12}$$

A comparison with similar boundary conditions (at $r = 1$) for the membrane model of the tube (Garg & Rouleau 1974, equation (9)) shows that the additional term $\bar{\eta}_r\, dV_z/dr$ appears for the present refined model.

The radial and axial components of the stress must also be continuous at the interface. Transforming to the location $r = 1$, we get for $\sigma \neq \frac{1}{2}$

$$\left.\begin{aligned} -p + 2D\bar{v}_r/R - \frac{\xi(1-\sigma)}{(1-2\sigma)}[(1-\sigma)\,D\bar{\eta}_r + \sigma(\bar{\eta}_r + k\bar{\eta}_z)] &= 0 \\ \frac{1}{R}\left[k\bar{v}_r + D\bar{v}_z + \bar{\eta}_r \frac{d^2V_z}{dr^2}\right] - \frac{\xi(1-\sigma)}{2}(k\bar{\eta}_r + D\bar{\eta}_z) &= 0 \end{aligned}\right\} \quad \text{at} \quad r = 1 \tag{13}$$

and for $\sigma = \frac{1}{2}$

$$\left.\begin{aligned} -p + 2D\bar{v}_r/R + \bar{\beta} - 0{\cdot}5\xi D\bar{\eta}_r &= 0 \\ \frac{1}{R}\left[k\bar{v}_r + D\bar{v}_z + \bar{\eta}_r \frac{d^2V_z}{dr^2}\right] - \frac{\xi}{4}(k\bar{\eta}_r + D\bar{\eta}_z) &= 0 \end{aligned}\right\} \quad \text{at} \quad r = 1. \tag{14}$$

At the outer surface of the tube it is assumed that the stress is related to the displacement by a dimensionless impedance matrix Z_{ij} $(i,j = 1,2)$, so that the dimensionless radial and axial components of the stress are $-Z_{11}\eta_r - Z_{12}\eta_z$ and $-Z_{21}\eta_r - Z_{22}\eta_z$ respectively. Owing to the continuity of these components at the outer surface $r = 1+h$, where h is the ratio of the thickness of the tube to the inner radius, the boundary conditions for $\sigma \neq \frac{1}{2}$ are

$$\left.\begin{aligned} \xi(1-\sigma)\,D\bar{\eta}_r + \left[\frac{\sigma\xi}{1+h} + \frac{Z_{11}(1-2\sigma)}{1-\sigma}\right]\bar{\eta}_r + \left[k\sigma\xi + \frac{Z_{12}(1-2\sigma)}{1-\sigma}\right]\bar{\eta}_z &= 0 \\ \left[k\xi + \frac{2Z_{21}}{1-\sigma}\right]\bar{\eta}_r + \xi D\bar{\eta}_z + \frac{2Z_{22}}{1-\sigma}\bar{\eta}_z &= 0 \end{aligned}\right\} \quad \text{at} \quad r = 1+h \tag{15}$$

and for $\sigma = \frac{1}{2}$ are

$$\left.\begin{aligned} 0{\cdot}5\xi D\bar{\eta}_r + Z_{11}\bar{\eta}_r + Z_{12}\bar{\eta}_z - \bar{\beta} &= 0 \\ (k\xi + 4Z_{21})\,\bar{\eta}_r + \xi D\bar{\eta}_z + 4Z_{22}\bar{\eta}_z &= 0 \end{aligned}\right\} \quad \text{at} \quad r = 1+h. \tag{16}$$

It may be noted that for an unconstrained tube $Z_{ij} = 0$, and that $Z_{ij} = aZ_{ij}^*/(\rho\mathscr{V}^2)$, where Z_{ij}^* is the dimensional counterpart of Z_{ij}.

For a given real value of ω (for spatial stability) or a given imaginary value of k (for temporal stability) and given values of the Reynolds number R and the tube parameters ξ, ζ, σ, h and Z_{ij}, the solution of (2) and (5) or (8) together with the boundary conditions (10), (12), (13) or (14), and (15) or (16) leads to an eigenvalue problem. The flow is considered to be spatially unstable when the disturbance grows with z and temporally unstable when it grows with time. In terms of k or ω, the flow will be spatially unstable when $k_r > 0$ and temporally unstable when $\omega_i > 0$.

3. Solution

The three coupled differential equations (2) for the fluid are solved by a numerical technique developed earlier by Garg & Rouleau (1974). In short, the eigenfunctions are expanded as a power series in r near $r = 0$. The series solution is terminated at a small but finite value of r and the solution is continued up to the inner wall of the tube by a fourth-order Runge–Kutta integration technique. This solution involves two complex constants, say U_1 and P_1.

Thus, if $(S_1, S_2, S_3) \equiv (\bar{v}_r, \bar{v}_z, \bar{p})$, the series expansion for each eigenfunction can be assumed to be of the form

$$S_j = r^{a_j}(S_{1j} + S_{2j} r^2 + S_{3j} r^4 + \ldots + S_{lj} r^{2(l-1)} + \ldots), \quad j = 1, 2, 3, \tag{17}$$

where the S_{lj} are complex constants with

$$(S_{11}, S_{12}, S_{13}) \equiv (V_1, U_1, P_1), \quad \text{etc.} \tag{18}$$

Substituting (17) into (2) and setting to zero the coefficient of r^α for each α in the resulting equations, the values of the a_j that satisfy the boundary conditions (10) at $r = 0$ are

$$(a_1, a_2, a_3) = (1, 0, 0), \tag{19}$$

and the recurrence relations for the V's, U's and P's are (Garg & Rouleau 1974)

$$U_{l+1} = \frac{1}{4l^2}\left[kRP_l - \gamma U_l - \frac{l-2}{l-1} kRU_{l-1}\right], \tag{20a}$$

$$V_{l+1} = \frac{-1}{2(l+1)} kU_{l+1}, \tag{20b}$$

$$P_{l+1} = \frac{1}{2Rl}[4l(l+1)V_{l+1} + \gamma V_l + kRV_{l-1}], \tag{20c}$$

where any term with either a zero or a negative subscript is set to zero, and where

$$\gamma = k^2 - R(k - i\omega) \tag{21}$$

and l is a positive integer.

P_1 and only one of U_1 and V_1 are independent owing to the relation

$$V_1 = -\tfrac{1}{2}kU_1. \tag{22}$$

Taking U_1 and P_1 to be independent, any eigenfunction can be expressed as a sum of two terms; for example, the pressure eigenfunction $\bar{p}(r)$ may be written as

$$\bar{p}(r) = p_1(r)\, U_1 + p_2(r)\, P_1. \tag{23}$$

This results in two sets of solutions (v_{r1}, v_{z1}, p_1) and (v_{r2}, v_{z2}, p_2) that are independent of each other, and must satisfy (2) independently.

The tube equations (5) or (8) are then solved for the displacements $\bar{\eta}_r$ and $\bar{\eta}_z$, and also for the finite pressure $\bar{\beta}$ in the case $\sigma = \frac{1}{2}$. The analytical solution of (5) (for $\sigma \neq \frac{1}{2}$) is

$$\bar{\eta}_r(r) = k\left[A\frac{J_1(qr)}{J_0(q)} + B\frac{Y_1(qr)}{Y_0(q)}\right] + m\left[C\frac{J_1(mr)}{J_0(m)} + D\frac{Y_1(mr)}{Y_0(m)}\right], \tag{24a}$$

$$\bar{\eta}_z(r) = -q\left[A\frac{J_0(qr)}{J_0(q)} + B\frac{Y_0(qr)}{Y_0(q)}\right] - k\left[C\frac{J_0(mr)}{J_0(m)} + D\frac{Y_0(mr)}{Y_0(m)}\right], \tag{24b}$$

and that of (8) (for $\sigma = \frac{1}{2}$) is

$$\bar{\eta}_r(r) = k\left[A\frac{J_1(qr)}{J_0(q)} + B\frac{Y_1(qr)}{Y_0(q)}\right] + k\left[C\frac{J_1(kr)}{J_0(k)} + D\frac{Y_1(kr)}{Y_0(k)}\right], \tag{25a}$$

$$\bar{\eta}_z(r) = -q\left[A\frac{J_0(qr)}{J_0(q)} + B\frac{Y_0(qr)}{Y_0(q)}\right] - k\left[C\frac{J_0(kr)}{J_0(k)} + D\frac{Y_0(kr)}{Y_0(k)}\right], \tag{25b}$$

$$\bar{\beta}(r) = -\zeta\omega^2\left[C\frac{J_0(kr)}{J_0(k)} + D\frac{Y_0(kr)}{Y_0(k)}\right]. \tag{25c}$$

Here J_0 and J_1 are Bessel functions of the first kind and orders zero and one, respectively; Y_0 and Y_1 are Bessel functions of the second kind and orders zero and one, respectively; and A, B, C and D are undetermined complex constants.

The six constants U_1, P_1, A, B, C and D must be evaluated in order to complete the solution. This is done with the help of six boundary conditions at the inner and outer wall of the tube. For tube material with $\sigma \neq \frac{1}{2}$, these boundary conditions are (12), (13) and (15), while for $\sigma = \frac{1}{2}$, they are (12), (14) and (16). This leads to six homogeneous linear equations for the six constants, so that for a non-trivial solution the determinant of the coefficient matrix must vanish. The vanishing of this determinant leads to the dispersion relation between k and ω, and enables the ratios of the six constants to be determined. When these ratios are used in the solution of the fluid and tube equations, they determine a solution of the problem, or a 'mode', up to a multiplicative constant. Available as roots of the dispersion relation, there are infinitely many values of the wavenumber k for spatial stability analysis or of the frequency ω for temporal stability analysis.

The problem then arises of the isolation of one or more of the infinite number of modes that may be unstable, i.e. for which the corresponding complex eigenvalue k has a positive real part for spatial analysis or for which the eigenvalue ω has a positive imaginary part for temporal analysis. This requires an investigation of a significant part of the complex k or ω plane. An eigenvalue search technique, developed by Garg & Rouleau (1972), was used for this purpose. Isolation of the eigenvalues was accomplished by dividing the region into smaller subregions until an eigenvalue was bracketed closely enough for an iterative technique to converge to it.

4. Computational procedure

The series solution for the fluid equations was applied in the region $0 \leqslant r \leqslant 0{\cdot}1$ and from 10 to 15 terms were required for convergence, the larger number of terms corresponding to Reynolds numbers of the order of 10^4. The convergence criterion for the series solution was that the ratio of the last term retained to the partial sum up

Case	E (MPa)	h	σ	ζ
1	10000	0·1	0·3	2·0
2	1000	0·1	0·3	2·0
3	1000	0·3	0·3	2·0
4	1000	0·1	0·5	2·0
5	1000	0·1	0·3	6·0

TABLE 1. Tube parameters.

to the last term but one should be less than 10^{-15}. The fourth-order Runge–Kutta method was used for numerical integration of the differential equations (2) over $0{\cdot}1 \leqslant r \leqslant 1$; the step size was generally taken to be 0·005. Double-precision algorithms were used to calculate the Bessel functions $J_n(z)$ (Scarton 1971) and $Y_n(z)$ (Garg 1976). Calculations were performed on an IBM 7044 computer that carried 17 digits in the double-precision mode.

5. Results

Results are presented here for the effect of purely elastic, unconstrained tubes (i.e. E real, $Z_{ij} = 0$) on the spatial stability of Poiseuille flow. For the tube material, density ratios ζ of 2·0 and 6·0, Poisson ratios σ of 0·3 and 0·5 and Young's moduli E of 10^3MPa ($1{\cdot}45 \times 10^5$psi) and 10^4MPa were chosen. The dimensionless tube thickness h was given the values 0·1 and 0·3 (see table 1). The fluid considered was glycerol at 30 °C ($\rho = 1260\,\mathrm{kg/m^3}$, $\nu = 3 \times 10^{-4}\,\mathrm{m^2/s}$), and the tube's inner radius a was taken to be 10 mm. As will be discussed later (see § 5.3), there is no loss of generality in fixing the values of ρ, ν and a since the results can be easily applied to any other combination of these parameters by using the dimensionless parameter ξ, defined by (4).

Recalling that all possible modes for the linear stability of Poiseuille flow in a rigid tube are stable (Garg & Rouleau 1972; Salwen & Grosch 1972; Gill 1973), it is interesting to note that elasticity of the tube introduces a mode (designated mode 1) that exhibits spatial instability ($k_r > 0$) and thus has a critical Reynolds number (corresponding to $k_r = 0$). There is *at least* one more mode, designated mode 2, that has no counterpart among the modes for flow in a rigid tube, but it is always stable. The behaviour of both these modes is dependent on the tube parameters as well as on the flow Reynolds number and disturbance frequency. Besides these modes, there is also a mode which is essentially the stable fluid-dynamic mode modified (only slightly) by the presence of the elastic wall. Since eigenvalues for this mode are very nearly the same as those for the least stable mode for a rigid tube (Garg 1971) and those for a membrane-like elastic tube (Garg & Rouleau 1974), they are not presented here.

5.1. *Behaviour of mode* 1

Figures 1–5 illustrate the variation of the spatial growth rate k_r and the phase velocity C_p ($= \omega/k_i$) with the Reynolds number R for mode 1 for various values of the disturbance frequency ω and for the five sets of tube parameters listed in table 1. These figures show that the curves for the spatial growth rate pass through a maximum that is dependent on the disturbance frequency and the tube parameters. Given

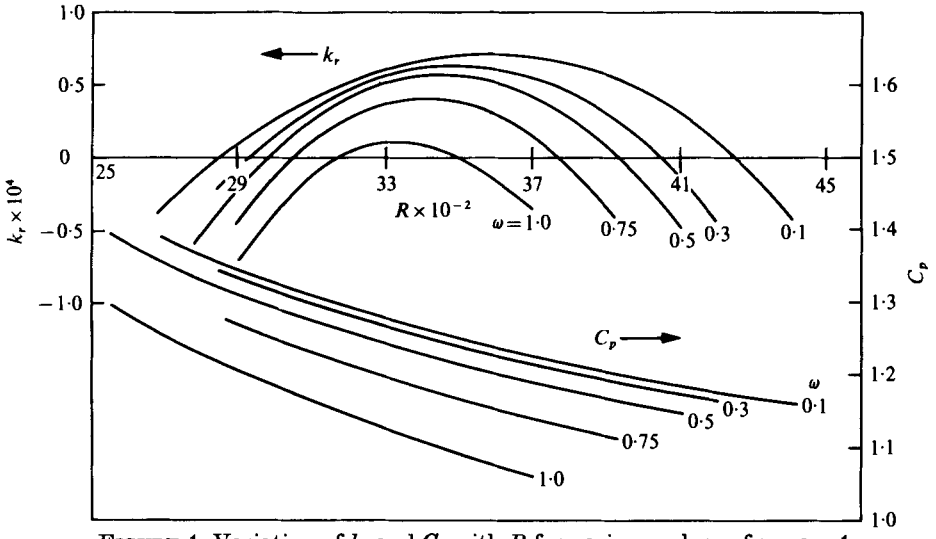

FIGURE 1. Variation of k_r and C_p with R for various values of ω: case 1 (mode 1, $E = 10^4$ MPa, $h = 0{\cdot}1$, $\sigma = 0{\cdot}3$, $\zeta = 2{\cdot}0$).

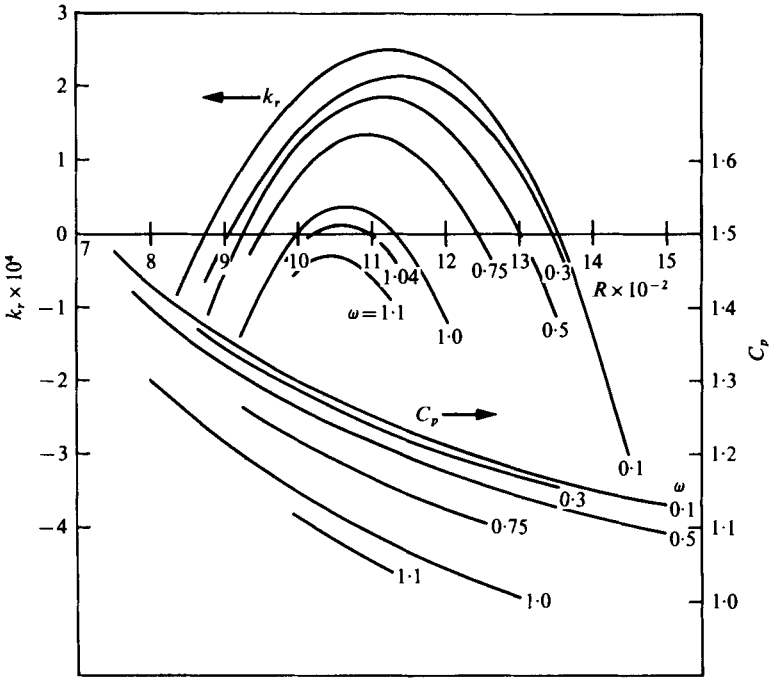

FIGURE 2. Variation of k_r and C_p with R for various values of ω: case 2 (mode 1, $E = 10^3$ MPa, $h = 0{\cdot}1$, $\sigma = 0{\cdot}3$, $\zeta = 2{\cdot}0$).

appropriate combinations of the flow Reynolds number and the tube parameters, the maximum growth rate increases as the frequency decreases. On comparing figures 1, 2 and 5, we find that the maximum growth rate $k_{r\max}$ increases as the Young's modulus E decreases or as the density ratio ζ increases. A comparison of figures 2 and 3 shows that $k_{r\max}$ decreases with increasing h for lower ω but increases with

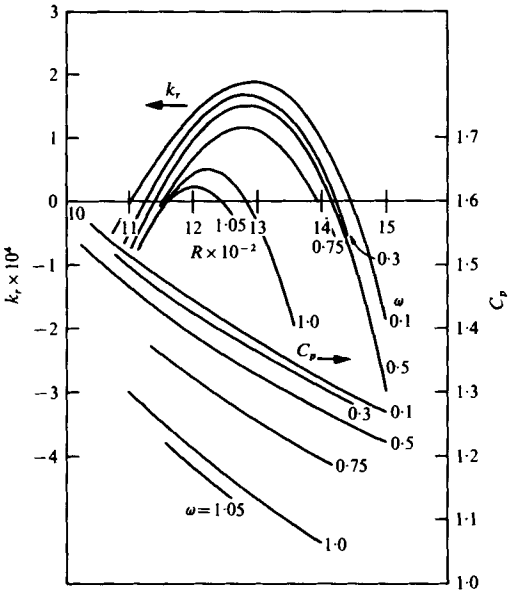

FIGURE 3. Variation of k_r and C_p with R for various values of ω: case 3 (mode 1, $E = 10^3$ MPa, $h = 0{\cdot}3$, $\sigma = 0{\cdot}3$, $\zeta = 2{\cdot}0$).

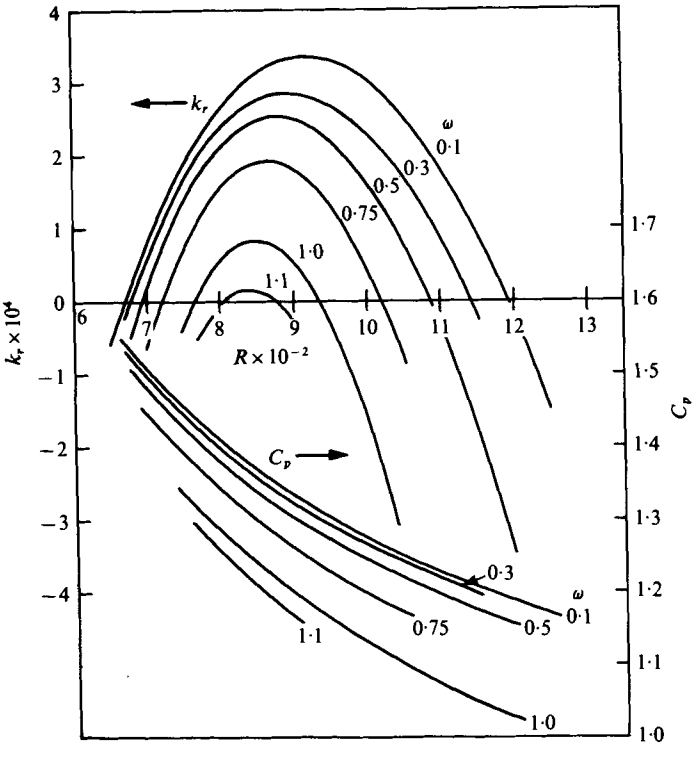

FIGURE 4. Variation of k_r and C_p with R for various values of ω: case 4 (mode 1, $E = 10^3$ MPa, $h = 0{\cdot}1$, $\sigma = 0{\cdot}5$, $\zeta = 2{\cdot}0$).

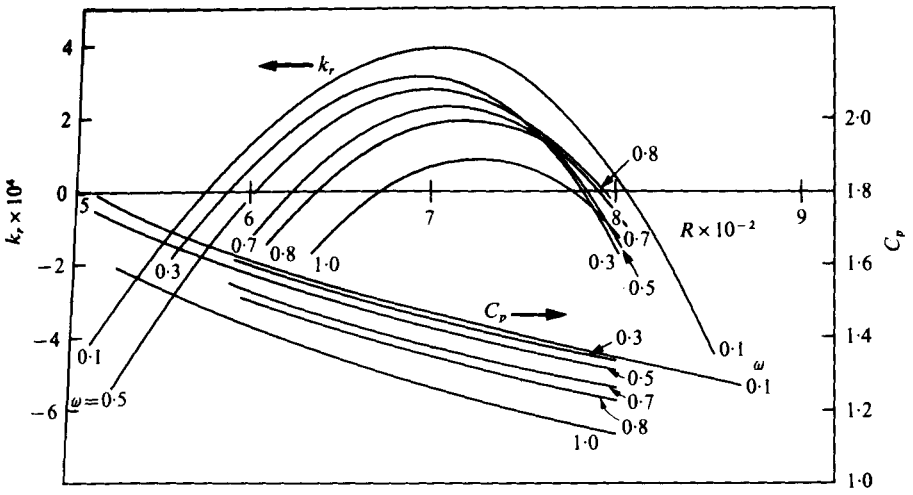

FIGURE 5. Variation of k_r and C_p with R for various values of ω: case 5 (mode 1, $E = 10^3$ MPa, $h = 0{\cdot}1$, $\sigma = 0{\cdot}3$, $\zeta = 6{\cdot}0$).

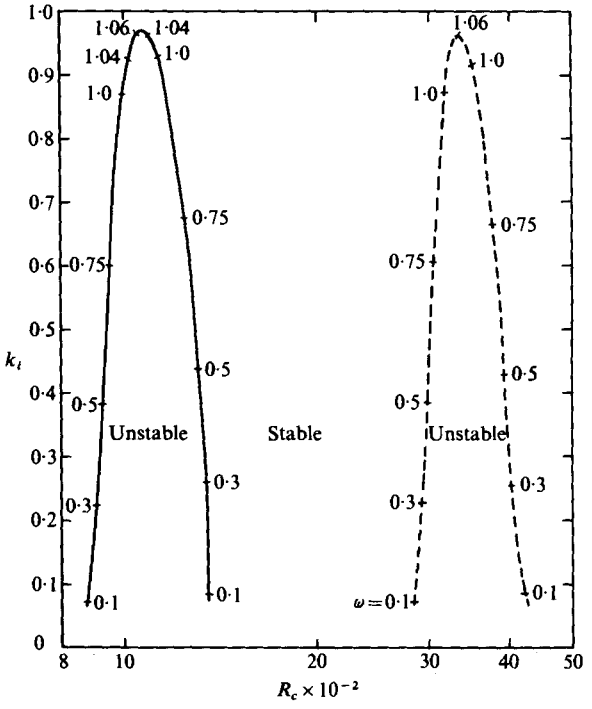

FIGURE 6. Neutral curves for two values of E ($h = 0{\cdot}1$, $\sigma = 0{\cdot}3$, $\zeta = 2{\cdot}0$). ——, $E = 10^3$ MPa; – – –, $E = 10^4$ MPa.

increasing h at higher frequencies, while a comparison between figures 2 and 4 shows that the maximum growth rate is higher for flow in an incompressible tube ($\sigma = 0{\cdot}5$) than for flow in a compressible tube ($\sigma = 0{\cdot}3$).

For all five cases, the phase velocity C_p lies between 1·0 and 2·0, and decreases either as the frequency ω or as the Reynolds number R increases. The values of C_p

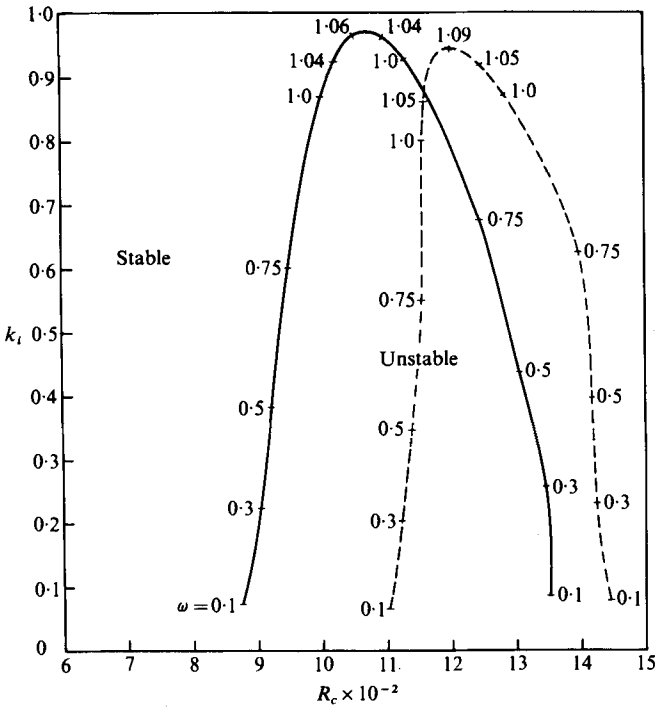

FIGURE 7. Neutral curves for two values of h ($E = 10^3$ MPa, $\sigma = 0{\cdot}3$, $\zeta = 2{\cdot}0$). ——, $h = 0{\cdot}1$; – – –, $h = 0{\cdot}3$.

greater than 1·0 imply that the dimensional phase velocity of the disturbance is greater than the maximum fluid velocity in the tube. Thus the motion derives primarily from the elastic vibrations in the tube but is influenced by the flow velocity. Therefore this mode, as well as mode 2, to be discussed later, corresponds to the class of elastic waves noted by Benjamin (1960, 1963) in his analyses of boundary-layer stability on an elastic surface; the instability of mode 1 is thus essentially a resonance effect. It may be noted that, for the results in figures 1–5, C_p varies such that $0{\cdot}5 < C_p/C_t < 1{\cdot}0$.

Since portions of the k_r, R curves that lie above the R axis ($k_r = 0$) correspond to instability of the flow, it can be observed that there is a range of Reynolds numbers for appropriate combinations of ω and the tube parameters for which the flow is unstable. For a given set of tube parameters, this range generally shrinks as the frequency of disturbance increases, and it nearly vanishes for $\omega \gtrsim 1{\cdot}1$ for the cases studied. This implies that, over the range of investigation, Poiseuille flow in an elastic tube is spatially stable to all infinitesimal axisymmetric disturbances of dimensionless frequency higher than about 1·1. The values of the critical Reynolds numbers R_c and the corresponding phase velocities are listed in table 2, while figures 6–9 show the neutral curves (k_i *vs.* R_c) for the various sets of tube parameter values, the disturbance frequencies being displayed over the curves. The parameters for these figures have been selected in such a way that the effect, on the neutral curve, of changing any one of the four tube parameters E, h, σ and ζ can be easily observed. Thus, while figure 6 provides a comparison between the neutral curves for two different values of E, figures 7, 8 and 9 do so for different values of h, σ and ζ respectively. It is instructive

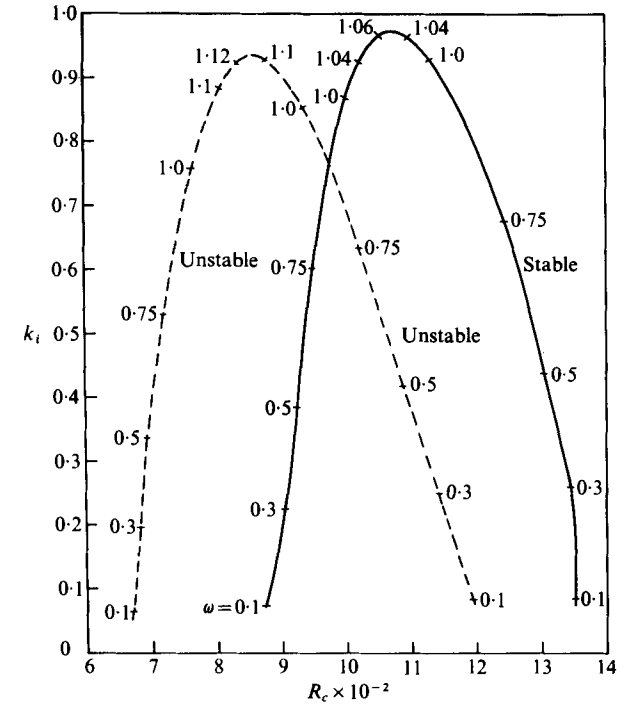

FIGURE 8. Neutral curves for two values of σ ($E = 10^3$ MPa, $h = 0{\cdot}1$, $\zeta = 2{\cdot}0$). ——, $\sigma = 0{\cdot}3$; – – –, $\sigma = 0{\cdot}5$.

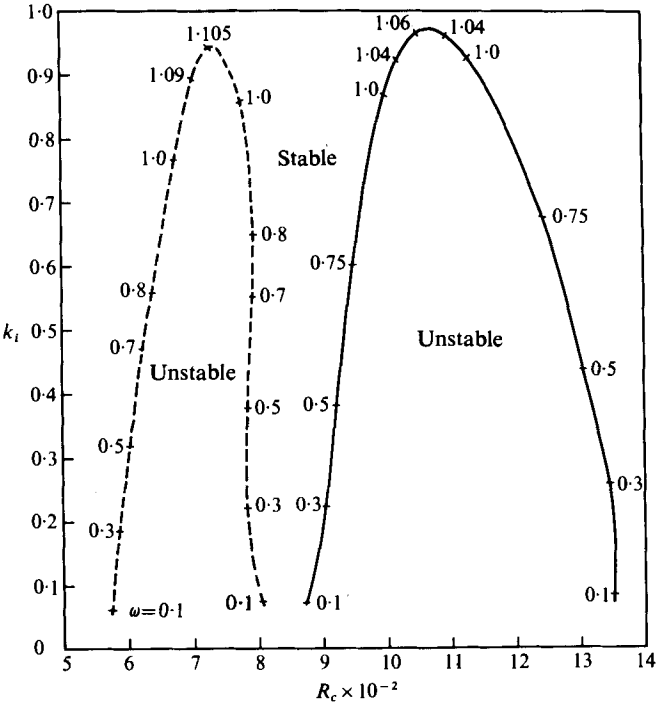

FIGURE 9. Neutral curves for two values of ζ ($E = 10^3$ MPa, $h = 0{\cdot}1$, $\sigma = 0{\cdot}3$). ——, $\zeta = 2{\cdot}0$; – – –, $\zeta = 6{\cdot}0$.

Frequency ω	Lower limit R_c	Lower limit C_p	Upper limit R_c	Upper limit C_p
		Case 1		
0·1	2852·08	1·3537	4250·24	1·1715
0·3	2927·13	1·3282	4047·39	1·1771
0·5	2979·63	1·2964	3932·98	1·1625
0·75	3049·72	1·2385	3771·80	1·1283
1·0	3172·79	1·1468	3487·34	1·0913
		Case 2		
0·1	874·98	1·3742	1352·87	1·1663
0·3	905·07	1·3412	1344·45	1·1583
0·5	923·30	1·3081	1304·02	1·1434
0·75	948·99	1·2480	1243·04	1·1097
1·0	998·41	1·1498	1130·27	1·0777
1·04	1019·69	1·1233	1096·46	1·0799
		Case 3		
0·1	1103·32	1·5134	1444·75	1·2994
0·3	1124·33	1·4805	1421·96	1·2972
0·5	1139·32	1·4366	1416·70	1·2647
0·75	1154·18	1·3567	1394·73	1·1981
1·0	1157·26	1·2464	1283·55	1·1443
1·05	1159·49	1·2169	1244·92	1·1435
		Case 4		
0·1	669·96	1·5424	1193·97	1·1889
0·3	677·61	1·5219	1142·47	1·2006
0·5	694·84	1·4841	1086·33	1·2004
0·75	721·13	1·4189	1020·81	1·1854
1·0	765·52	1·3176	936·01	1·1709
1·1	806·41	1·2482	877·37	1·1838
		Case 5		
0·1	575·20	1·6611	805·98	1·3364
0·3	587·64	1·6222	780·86	1·3576
0·5	602·32	1·5684	783·14	1·3263
0·7	623·37	1·4901	791·23	1·2685
0·8	636·80	1·4391	793·30	1·2323
1·0	672·49	1·3052	774·52	1·1624

TABLE 2. Values of R and C_p for neutral spatial stability ($k_r = 0$).

Case	R	ω_c	C_p
1	3320·0	1·05764	1·0989
2	1050·0	1·06133	1·0975
3	1200·0	1·09148	1·1551
4	835·0	1·12075	1·2145
5	700·0	1·08742	1·2175
5	725·0	1·10489	1·1692

TABLE 3. Values of ω and C_p for neutral spatial stability ($k_r = 0$).

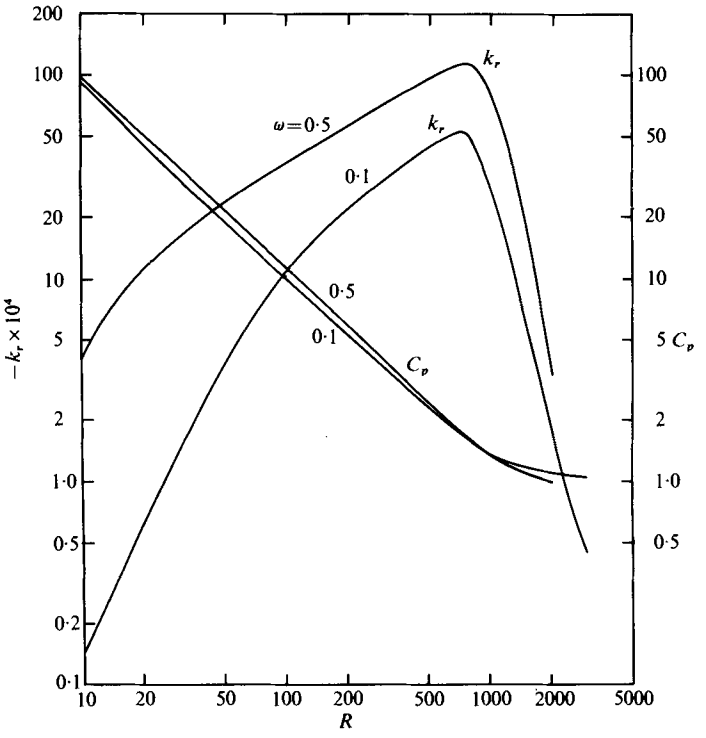

FIGURE 10. Variation of k_r and C_p with R for mode 2 ($E = 10^3$ MPa, $h = 0{\cdot}1$, $\sigma = 0{\cdot}3$, $\zeta = 6{\cdot}0$).

to note that both the lower and the upper critical Reynolds numbers vary almost as the square root of the Young's modulus for the tube material. This is to be expected since $E \propto R^2$ [see (4)]. Since the phase velocity corresponding to the neutral curves is almost unity, the curves of ω *vs.* R_c look very similar to those presented here.

Table 3 lists some critical frequencies and phase velocities for Reynolds numbers close to the peak points on the neutral curves in figures 6–9.

5.2. *Behaviour of mode* 2

In contrast to mode 1, for which the flow is unstable owing to the elasticity of the tube material, mode 2 is always stable. Therefore only a few eigenvalues corresponding to this mode were computed. These are displayed in figure 10 in terms of k_r, R and C_p, R curves for $\omega = 0{\cdot}1$ and $0{\cdot}5$. It can be observed that, as R increases, this mode tends to become neutrally stable while its phase velocity approaches unity. In addition, the k_r, R curves exhibit a minimum (note that $-k_r$ has been plotted *vs.* R), which implies that this mode is 'most stable' for a particular Reynolds number. Also, a simple calculation shows that the ratio of C_p to C_t is of the order of unity, C_p being less than C_t at low Reynolds numbers but greater than C_t at high Reynolds numbers.

5.3. *Effect of* a, ρ *and* ν

It is imperative to describe the effect of changes in the dimensional variables a, ρ and ν, since they enter the dimensionless parameters R, ζ and ξ but were kept at the

previously given constant values during the investigation. If the tube's inner radius a were doubled but R and h were kept constant, the centre-line velocity $\mathscr{V}$ would be halved, and, in order to keep the same value of the dimensionless parameter ξ, the Young's modulus E should be reduced by a factor of 4 [see (4)]. Thus, for a tube with twice the previous inner radius all the above results would hold for values of E one-quarter of those indicated. Similarly, for twice the fluid density but for the same value of ζ, E should be doubled, and for twice the fluid viscosity but with R constant, E should be quadrupled for all the previous results to hold.

Extending these arguments to find the critical Reynolds number for flow of glycerol at 30 °C through a 20 mm I.D. steel tube of thickness 1 mm, we find that the tube parameters ζ, h, and σ for case 5 (see table 1) are the appropriate ones. For case 5, $\zeta = 6{\cdot}0$ corresponds to $\rho_w = 7560\,\mathrm{kg/m^3}$ while for steel $\rho_w = 7750\,\mathrm{kg/m^3}$. Thus, to keep ζ fixed at 6·0 for steel, ρ should be $1292\,\mathrm{kg/m^3}$, so that results for case 5 would hold for $E = 1{\cdot}025 \times 10^3\,\mathrm{MPa}$ if $\rho = 1292\,\mathrm{kg/m^3}$. Since for steel $E = 2 \times 10^5\,\mathrm{MPa}$, and since R_c varies almost as $E^{\frac{1}{2}}$, we find that the critical Reynolds numbers listed in table 2 for case 5 should be multiplied by a factor of about 14 in order to apply to flow in a steel tube as described above.

6. Conclusions

From these results, it seems likely that the difference between the predictions of linear stability theory for rigid-pipe flow as compared with channel flow is due to the pipe flow being completely enclosed by a solid boundary whereas the channel flow is only partially confined. Elasticity of the pipe wall tends to ease the confinement of Poiseuille flow, leading to instability even to infinitesimal axisymmetric disturbances over a range of flow Reynolds numbers and disturbance frequencies. The flow is, however, stable if the frequency exceeds a certain upper limit, and also if the Reynolds number is either less than a lower limit or more than an upper limit. Both the lower and the upper critical Reynolds numbers vary with the tube parameters E, h, σ and ζ, but the critical frequency is almost invariant and is about 1·1 for the cases studied. It is also found that both the critical Reynolds numbers vary almost as the square root of the Young's modulus of the tube material.

The phase velocity of growing disturbances is greater than the maximum velocity of the Poiseuille flow and is of the same order of magnitude as the speed of sound in the tube material. This indicates that instability of the flow is caused by the elastic waves in the tube, modified by the presence of fluid flow.

REFERENCES

BENJAMIN, T. B. 1960 *J. Fluid Mech.* **9**, 513.

BENJAMIN, T. B. 1963 *J. Fluid Mech.* **16**, 436.

BENJAMIN, T. B. 1964 *Proc. 11th Int. Cong. Appl. Mech., Munich*, p. 109.

COX, R. H. 1969 *J. Biomech.* **2**, 251.

DEARMOND, R. P. & ROULEAU, W. T. 1972 *J. Basic Engng, Trans. A.S.M.E.* **94**, 811.

GARG, V. K. 1971 Ph.D. thesis, Carnegie-Mellon University, Pittsburgh. (See also *University Microfilms, Ann Arbor, Michigan*, no. 71-24, p. 852.)

GARG, V. K. 1976 Submitted to *Comp. J.*

GARG, V. K. & ROULEAU, W. T. 1972 *J. Fluid Mech.* **54**, 113.
GARG, V. K. & ROULEAU, W. T. 1974 *Phys. Fluids* **17**, 1103.
GILL, A. E. 1973 *J. Fluid Mech.* **61**, 97.
HAINS, F. D. & PRICE, J. F. 1962*a* *Phys. Fluids* **5**, 365.
HAINS, F. D. & PRICE, J. F. 1962*b* *Proc. 4th U.S. Nat. Cong. Appl. Mech.* p. 1263.
LANDAHL, M. T. 1962 *J. Fluid Mech.* **13**, 609.
LIN, T. C. & MORGAN, G. W. 1956 *J. Acoust. Soc. Am.* **28**, 1165.
LOVE, A. E. H. 1944 *A Treatise on the Mathematical Theory of Elasticity*, 4th edn, § 99, p. 193. Dover.
MILES, J. W. 1957 *J. Fluid Mech.* **3**, 185.
RUBINOW, S. I. & KELLER, J. B. 1971 *J. Acoust. Soc. Am.* **50**, 198.
SALWEN, H. & GROSCH, C. E. 1972 *J. Fluid Mech.* **54**, 93.
SCARTON, H. A. 1971 *J. Comp. Phys.* **8**, 295.